Improve PV and energy systems' capacity to support voltage with FLC-based MPPC

DHARAVATH RAMESH[1]|MADDHI SARITHA[2]|KOMMU RAMESH[3]|MADISHETTI PRIYANKA SOUMYA[4]

1&2 Assistant Professor, EEE department, Brilliant Grammar School Educational Society's Group of Institutions, Hyderabad, TS.

3&4 UG SCHOLARS, EEE department, Brilliant Grammar School Educational Society's Group of Institutions, Hyderabad, TS.

ABSTRACT: Historically, photovoltaic (PV) inverters have been controlled for voltage and power using the cascaded control approach, which consists of an inner modern loop and an outer voltage loop. However, this method's capacity to regulate power is severely limited. The voltage upward push/drop has become a major issue that has a detrimental effect on grid stability and power quality because to the rapidly increasing penetration of PV strength era structures within the distribution community. In order to provide ancillary services, PV inverters greatly desire flexible strength regulation. In order to regulate and coordinate the dc-dc converter and inverter for grid-linked PV constructions with energy storage systems (ESS), this research suggests a unique model predictive power control (MPPC) scheme. MPPC can assist the energy grid in maintaining high voltage and frequency and enhancing the strength of the system by controlling the dc-bus voltage and the flows of active and reactive power. A PV-ESS device has undergone numerical simulation results to confirm the usefulness and efficiency of the suggested control approach.

KEYWORDS: PI controller, model predictive power control (MPPC), energy storage systems (ESS).PV panels.

I.INTRODUCTION:

For environment protection by reducing the greenhouse gas emissions, numerous government policies have been established to encourage the use of renewable energy sources. As one of the most promising renewable energy sources, the global solar photovoltaic (PV) power capacity has been increasing rapidly. According to the International Energy Agency (IEA), by 2050, the solar PV power generation will contribute 16% of the world’s electricity, and 20% of that capacity will come from residential installations [1].

Because of the intermittent power generation, PV systems must be equipped with energy storage systems (ESS) to achieve smooth power flows [2], and connected to the power grid for reliable power supply. In grid integration, the power electronic converter plays an important role to interface between the power grid and renewable energy sources [3], [4]. Fig.1 shows a typical PV-ESS configuration. The boost converter is used to achieve maximum power point tacking (MPPT) for the PV panels. The bidirectional dc-dc converter is controlled to absorb excess energy by charging or supply additional energy by discharging the ESS. The grid-connected inverter converts the dc-bus voltage into the ac grid voltage.

For PV system control, the cascaded linear control method has been widely used for decades [5]. This control structure requires multiple feedback loops and PWM modulation, resulting in

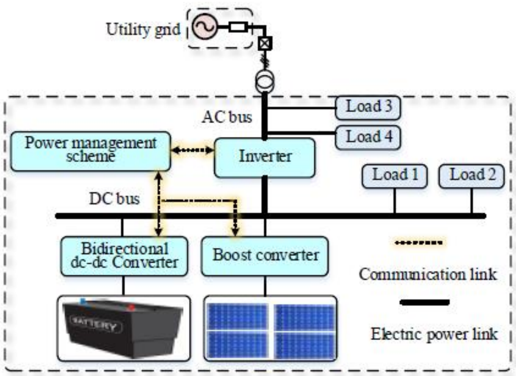

Fig.1. a PV-ESS configuration

Relatively slow dynamic response. In a practical PV power plant, the fluctuating PV panel output can cause oscillations in the dc-bus voltage, and deteriorate the power quality on the ac side. As a result, the traditional cascaded control is ineffective to deal with this fluctuation. Another concern is the power flow between the PV system and utility grid, which is usually handled by the grid-connected inverters. Traditionally, the cascaded feedback loops with PID controllers are adopted to control the ESS dc-dc converter and the grid-connected inverter [6]-[11]. To regulate the ESS charging or discharging current, an inner current control loop is commonly employed [6]-[8]. For the grid-connected inverter, an outer voltage loop is used to maintain the dc-bus voltage with the *d*-axis current reference as the output. In the inner current loop, the *d*-axis current is controlled to regulate the active power flow, and the *q*-axis current to regulate the reactive power flow [9]-[11]. Usually, the *q*-axis current reference is set to zero for unity power factor operation. In this conventional control strategy, the flexible power regulation capability is limited because both the active and reactive power flows between the PV system and the grid cannot be controlled directly. With the fast increasing penetration of PV systems in the distribution network, the voltage rise/drop has become a problem which impacts negatively on the power quality and grid stability [12], [13]. Therefore, flexible power regulation is highly desired for PV inverters to provide ancillary services.

To achieve flexible power regulation, the PV system control method must be modified to control the active and reactive power flows injected in the point of common coupling (PCC) with the grid. In the past few years, the model predictive control (MPC) scheme, in which the optimal switching state of power converter is determined according to a specified cost function, has been adopted to obtain better converter performance than PID control.

II.SYSTEM CONFIGARATION:

FROM fig.1 in this paper, a new model predictive power control (MPPC) strategy is proposed to control and coordinate the bidirectional dc-dc converter and inverter in PV-ESS systems as shown in Fig.1. The active power is chosen as the control objective for the bidirectional dc-dc converter and both the active and reactive power flows as the control objectives of the grid-connected inverter. The MPPC method in ESS can smooth the PV fluctuating output and maintain the stability of dc-link voltage, and the MPPC scheme for the inverter can control flexibly the power flow between the PV-ESS system and the utility grid, such that the PV-ESS system can support the grid by compensating the voltage to a certain degree.

Currently, there are several reports devoted to the MPC-based system-level stability. However, to date, to the authors' best knowledge, it is still an open question about the robustness and stability analysis of device-level MPC control of power converters. Carrying out extensive simulations under different key control parameters is an effective way to evaluate the robustness and stability of the designed MPC controllers. In this study, the robustness and stability are estimated by gradually varing filter settings. It is proved that the proposed MPPC scheme is highly stable and robust, as well as invulnerable to parameter variations. After that, the system performance are also examined with a longer-horizon prediction and compared with existing MPC methods. The results show that the proposed MPPC scheme is indeed feasible and effective using only one-step prediction. In addition, the proposed MPPC scheme is superior to existing MPC combinations in terms of maintaining a stable dc-bus voltage and providing a flexible power regulation.

III.PROPOSED CONTROL STRATEGY

A. Control of Bidirectional Buck-boost Converters

Traditionally, in a grid-connected PV system, the dc-bus voltage is maintained by using an inverter, and a buck-boost converter is used to regulate the ESS charging/discharging current to smooth the PV output. This control structure limits the flexible power regulation capability of PV-ESS system because the active and reactive power flows between the PV-ESS system and the grid cannot be controlled directly and flexibly. The question has now become whether it is possible to maintain the dc-bus voltage by controlling the dc-dc buck-boost converter rather than the inverter so that the control freedom of the inverter on the bidirectional active and reactive power flows can be fully explored?

To provide a positive answer to the above question, an in-depth analysis of the system model is performed. Fig.3.1 shows the ESS schematic configuration, where a dc-dc converter is used to interface the low voltage (LV) bus, which is connected to the battery, and the high voltage (HV) bus, also known as the dc-link. Fig.3.2 shows the equivalent circuits of (a) boost and (b) buck modes, respectively. If *S*2 is switching (1 or 0) as a main process and *S*1 is complementary, it operates in the boost mode (Fig.3(a)). The battery supplies power to the dc-link through discharging. On the contrary, if *S*1 is switching (1 or 0) as a main process and *S*2 is complementary, it operates in the buck mode (Fig.3(b)). The battery is charged with absorbing power from the dc-link.

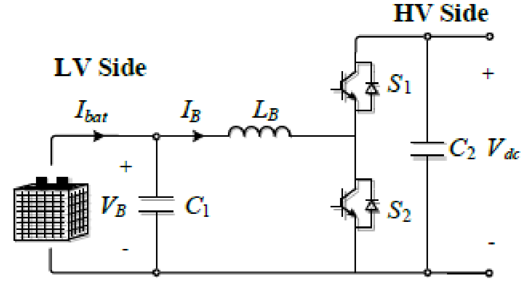

Fig.3.1. Schematic diagram of the ESS.

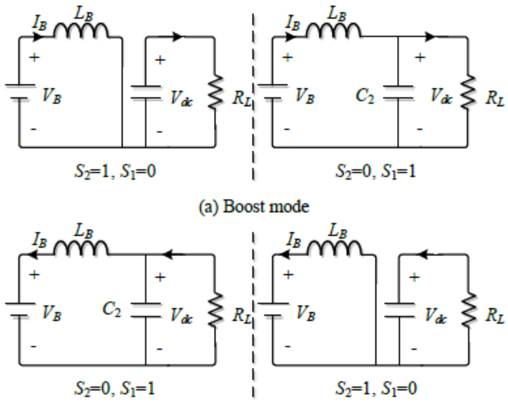

(b) Buck mode

Fig.3.2. Equivalent circuits of (a) boost and (b) buck modes.

In the boost operation, the circuit model is expressed as

$$\begin{cases} S_2 = 1, S_1 = 0: \ L_B \dfrac{dI_B}{dt} = V_B \\ S_2 = 0, S_1 = 1: \ L_B \dfrac{dI_B}{dt} = V_B - V_{dc} \end{cases} \quad (1)$$

The discrete-time model for a sampling time Ts can be written as:

$$\begin{cases} S_2 = 1, S_1 = 0: \ I_B(k+1) = \dfrac{T_s}{L_B} V_B(k) + I_B(k) \\ S_2 = 0, S_1 = 1: \ I_B(k+1) = \dfrac{T_s}{L_B}(-V_{dc}(k) + V_B(k)) + I_B(k) \end{cases} \quad (2)$$

Correspondingly, the discrete-time models of the buck operation can be described as:

$$\begin{cases} S_2 = 0, S_1 = 1: I_B(k+1) = \dfrac{T_s}{L_B}(V_{dc}(k) - V_B(k)) + I_B(k) \\ S_2 = 1, S_1 = 0: I_B(k+1) = -\dfrac{T_s}{L_B} V_B(k) + I_B(k) \end{cases} \quad (3)$$

Since the battery charging and discharging processes depend fundamentally on the current, it is necessary to know the relationship of currents in the entire system. Fig.3.3 illustrates the currents flowing between the renewable energy sources (RES), which is PV in this case, ESS and the rest of the microgrid (ROM).

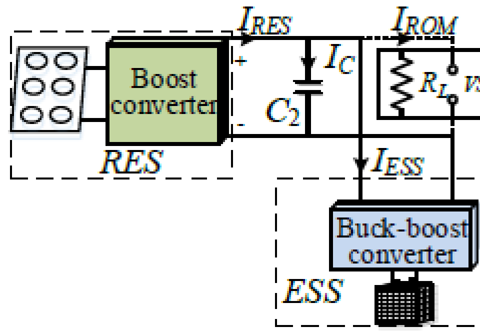

Fig.3.3. Currents flowing in the microgrid.

By the Kirchoff's current law (KCL), one obtains

$$I_{ESS} = I_{RES} - I_C - I_{ROM} \quad (4)$$

Where *IESS* is the charging/discharging current of ESS (assuming charging as the positive direction), *IROM* the current flowing into the dc loads and the dc-ac voltage source inverter (VSI), *IRES* the current from the renewable (PV) energy source, and *IC* the dc-bus capacitor current. Therefore, the required power from ESS to keep the system power balance can be determined by

$$P_{ESS}^{*} = \left| I_{ESS} \cdot V_{dc}^{*} \right| \quad (5)$$

where V_{dc}^{*} is the dc-bus voltage reference. Conforming to the capacitor characteristic, the dc-bus capacitor current at the (k+1)th time step can be predicted by

$$I_C(k+1) = \frac{1}{N}\left(\frac{C_2}{T_s}(V_{dc}^{*} - V_{dc}(k))\right) \quad (6)$$

where N is an integer coefficient utilized to limit the capacitor current [15], $C2$ the capacitance of dc-bus capacitor, and $Vdc(k)$ the dc-bus voltage at the kth time step. Substituting (6) into (4) and assuming that *IRES* and *IROM* are unchanged during a short period *Ts*, *IESS* at the next sampling instant can be predicted as

$$I_{ESS}(k+1) = I_{RES}(k) - \frac{1}{N}\left(\frac{C_2}{T_s}(V_{dc}^{*} - V_{dc}(k))\right) - I_{ROM}(k) \quad (7)$$

With the predicted ESS current, the required power of ESS in the next control instant can be computed by (5) and (7) as

$$P_{ESS}^{*}(k+1)=\left|\left[I_{RES}(k)-\frac{1}{N}\left(\frac{C_2}{T_s}(V_{dc}^{*}-V_{dc}(k))\right)-I_{ROM}(k)\right]\cdot V_{dc}^{*}\right| \quad (8)$$

Since the change of battery voltage is relatively slow and the battery output current is equal to its inductor current, the battery output power can be predicted as

$$P_{bat}(k+1)=\left|I_B(k+1)\cdot V_B(k)\right| \quad (9)$$

To keep the power balance, the required power of ESS should be provided/absorbed by the battery. Therefore, the cost function of MPPC in ESS can be formulated as

$$\begin{gathered} J_P=\left|P_{ESS}^{*}(k+1)-P_{bat}(k+1)\right| \\ s.t.\ SOC_{min}\le SOC\le SOC_{max},\ I_{bat}\le\left|I_{bat\_rated}\right| \end{gathered} \quad (10)$$

Where *SOC* is the state of charge defined as

$$SOC=1-\frac{1}{Q_0}\int_0^t I_{bat}(t)dt\ ,$$

Where *Q*0 is the total amount of charge stored in a battery in Ah, *t* the time in seconds, and *Ibat*(*t*) the battery current in A. Now it can be seen that the measurement and prediction of the dc-bus voltage are actually reflected in (8), and the control of the actual dc-bus voltage to track the reference is implemented in (10).

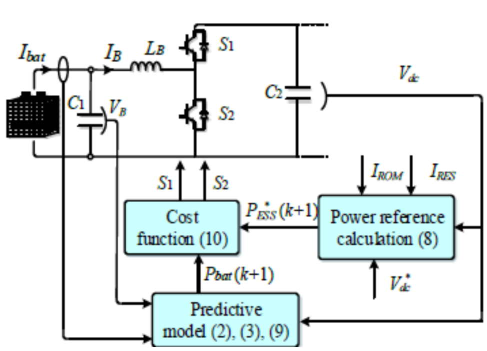

Fig.3.4. Block diagram of MPPC to control the dc-dc bidirectional converter

Fig.3.4 shows the proposed MPPC strategy for ESS. The required ESS power can be calculated jointly from the renewable energy source output current, *IRES*, the dc load current and inverter input current, *IROM*, the actual dc-bus voltage, *Vdc*, and the reference dc-bus voltage, *Vdc**, by (8). Simultaneously, the battery voltage and current and the actual dc-bus instant voltage will be used to predict the battery current *IB*(*k*+1), producing two possible values of *Pbat*(*k*+1) by (2), (3) and (9). The optimal switching state that minimizes (10) will be chosen to control the buck-boost converter. Thus, the dc-bus voltage can be maintained stable as the common dc-link for PV-ESS and as the dc input for the dc-ac converter.

B. Control of Grid-Connected Inverters

Since the dc-bus voltage can be regulated by using the bidirectional buck-boost dc-dc converter of the ESS, the grid-connected inverter or the dc-ac converter can now be endowed with more control flexibility to provide ancillary services in the grid side. As to the dc-ac converter, depending on the switching ON/OFF states, it has eight voltage vectors for its outputs. Their complex forms can be described as

$$V_i=\begin{cases}\frac{2}{3}V_{dc}^{*}e^{j(i-1)\frac{\pi}{3}} & (i=1,2,\cdots,6)\\ 0 & (i=0,7)\end{cases} \quad (11)$$

Fig.3.5 presents the ac-side system. The mathematical model of dc-ac converter can be expressed in the space phasor form as

$$\boldsymbol{V}_i=\boldsymbol{V}_g+\boldsymbol{I}_f R_f+L_f\frac{d\boldsymbol{I}_f}{dt} \quad (12)$$

where *Vi* and *Vg* are the voltage vectors of the converter and the grid, respectively, *If* is the inductor current vector, *Rf* the equivalent resistance, and *Lf* the filter inductance.

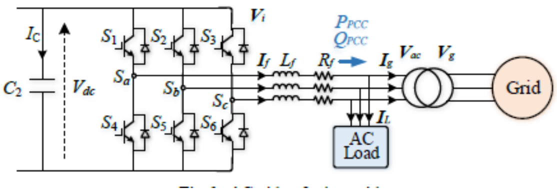

Fig.3.5. AC-side of microgrid

The output active and reactive power flows through the dc-ac converter into the ac common bus (*Vac*) or the PCC can be calculated by (in the *αβ*-plane)

$$P_{PCC} = \frac{3}{2}\mathrm{Re}\{V_g \bar{I}_f\} = \frac{3}{2}\left(V_{g\alpha} I_{f\alpha} + V_{g\beta} I_{f\beta}\right) \qquad (13)$$

$$Q_{PCC} = \frac{3}{2}\mathrm{Im}\{V_g \bar{I}_f\} = \frac{3}{2}\left(V_{g\beta} I_{f\alpha} - V_{g\alpha} I_{f\beta}\right) \qquad (14)$$

where ‾ represents the complex conjugate, Re{} the real component, and Im{} the imaginary component. The active and reactive power flows at the end of each sampling period can be predicted by (11) - (14) as [21]

$$P_{PCC}(k+1) = T_s\left[-\frac{R_f}{L_f}P_{PCC}(k) - \omega Q_{PCC}(k) + \frac{3}{2L_f}\left(\left|V_g\right|^2 - \mathrm{Re}\left(V_g \bar{V}_i\right)\right)\right] + P_{PCC}(k) \qquad (15)$$

$$Q_{PCC}(k+1) = T_s\left[\omega P_{PCC}(k) - \frac{R_f}{L_f}Q_{PCC}(k) - \frac{3}{2L_f}\mathrm{Im}\left(V_g \bar{V}_i\right)\right] + Q_{PCC}(k) \qquad (16)$$

where *ω* is the grid frequency in radians. In the case of grid-tied mode, the active and reactive power flows are the control objectives, resulting in the following cost function to be minimized to assess the effects of each voltage vector on *PPCC* and *QPCC* as

$$J_P = \left(P_{ref} - P_{PCC}(k+1)\right)^2 + \left(Q_{ref} - Q_{PCC}(k+1)\right)^2 \qquad (17)$$

The proposed MPPC strategy for the dc-ac converter is presented in Fig.3.6. The grid voltage, *Vg*, the inductor current vector, *If*, and the converter voltage vectors, *Vi*, are used to predict the next instant active and reactive powers. The selected switching states that can minimize (17) with the input active power reference *Pref* and reactive power reference *Qref* are sent to the dc-ac converter to realize the control. A positive *Pref* means that the active power flow from the grid to the dc-bus, and vice versa. The positive direction of the reactive power reference, *Qref*, is defined similarly. By specifying flexible *Pref* and *Qref* in a certain range, the PV-ESS can support and compensate the grid voltage to some degree.

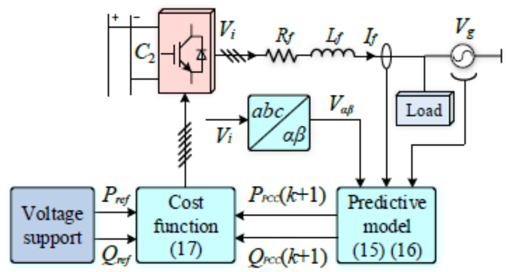

Fig.3.6. Block diagram of MPPC for the dc-ac converter connected to the grid.

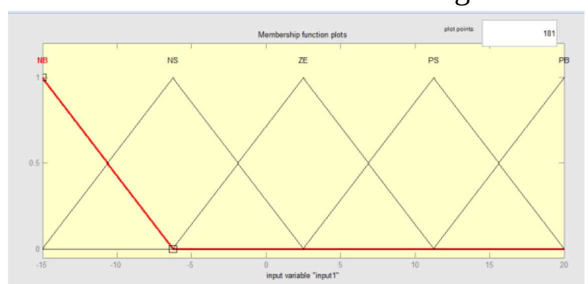

Input-1

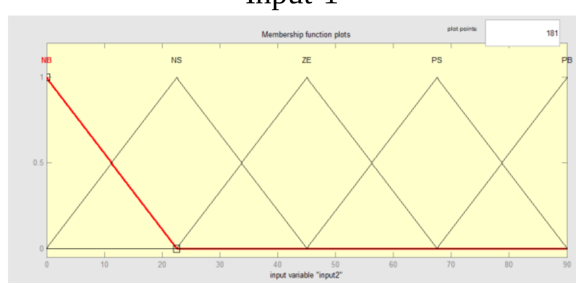

Input-2

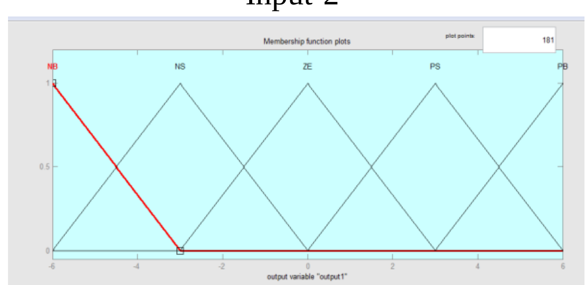

Output

IV.SIMULATION RESULTS:

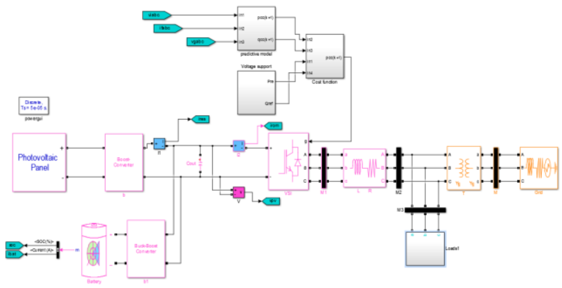

Fig 4.1Proposed simlink system

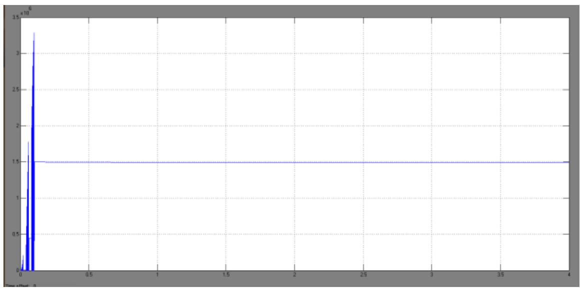

A

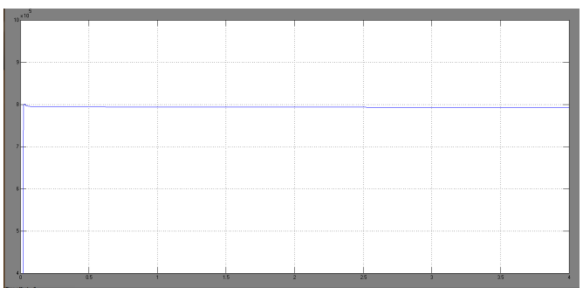

B

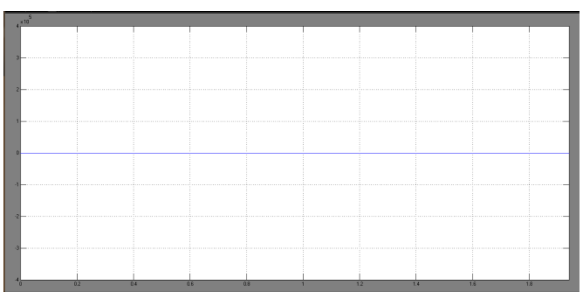

C

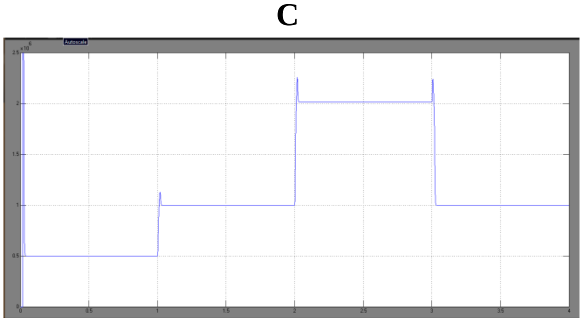

D

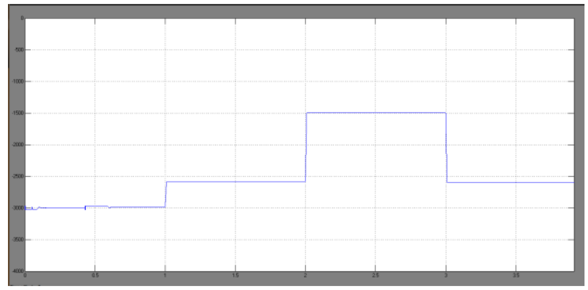

E

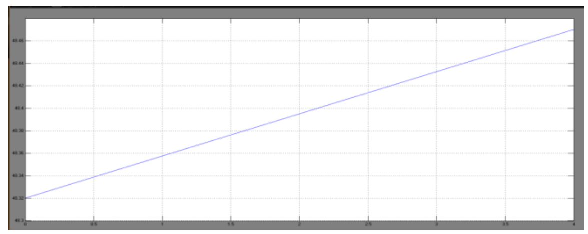

F

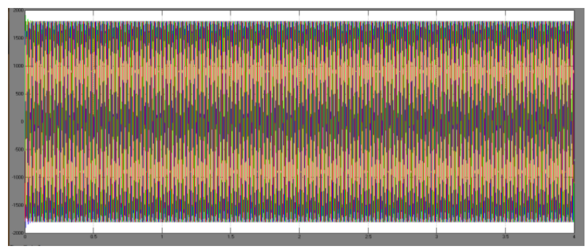

G

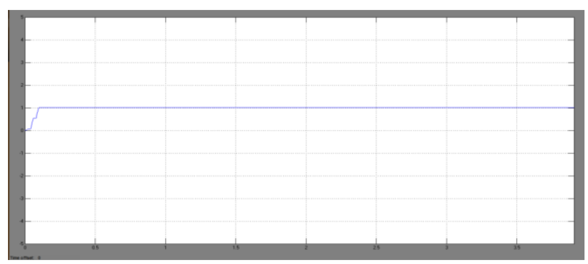

H

The performance of MPPC for dc-dc bidirectional converter under variable load demand condition: (a) PV power, (b) active power at PCC, (c) reactive power at PCC, (d) load power, (e) battery current, (f) SOC, (g) the current flowing between utility grid and PV-ESS system, (h) dc-bus voltage**.**

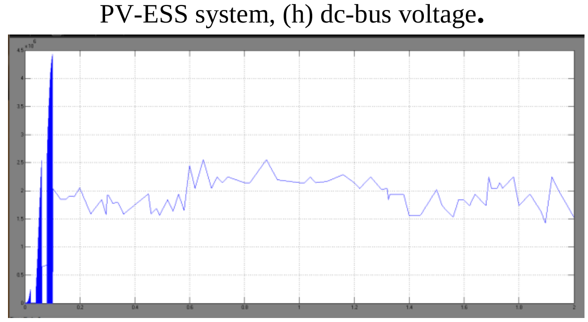

A

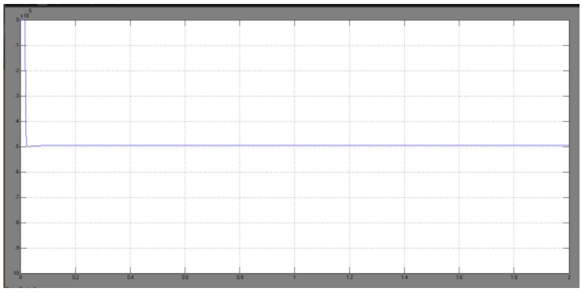

B

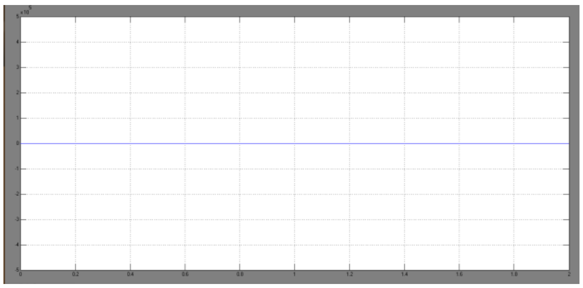

C

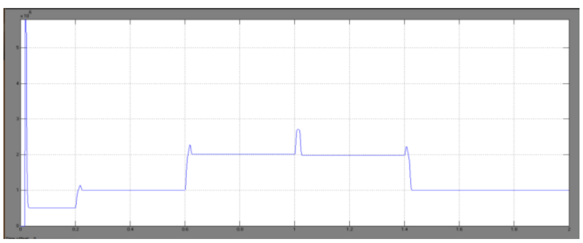

D

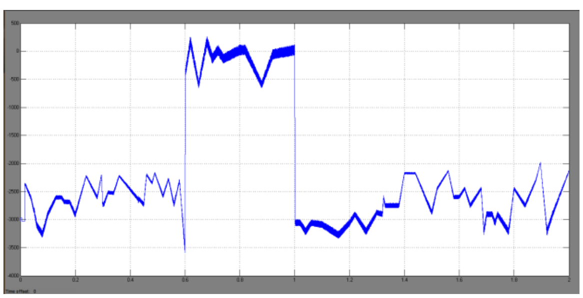

F

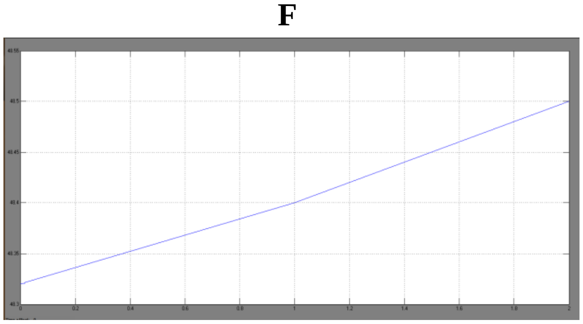

G

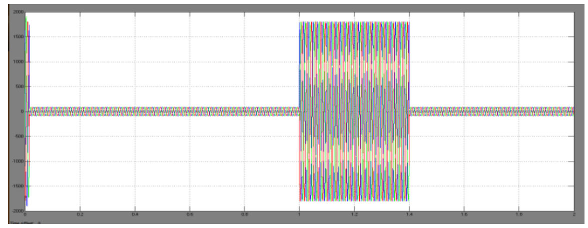

H

The performance under real-world fluctuant PV output using proposed method: (a) PV power, (b) active power at PCC, (c) reactive power at PCC, (d) load power, (e) battery current, (f) SOC, (g) the current flowing between utility grid and PV-ESS system, (h) dc-bus voltage.

V.CONCLUSION

An MPC-based MPPC method for a micro grid with PV-ESS systems is proposed in this research. When the dc-bus is linked to the utility grid, the MPPC and FLC controllers for the dc-dc bidirectional converter work to maintain a steady and reliable dc-bus voltage in order to mitigate the impact of the variable PV output, which would otherwise alter the grid voltage. Stable dc- and ac-bus voltages, even in the presence of erroneous power tracking, allow for flexible power distribution. A voltage support technique is created to make up for and restore the voltage dips brought on by varying loads. Numerical simulation findings for various scenarios validate the suggested MPPC method.

REFERENCES

[1] https://www.iea.org

[2] J. M. Guerrero, J. C. Vasquez, J. Matas, L. G. de Vicuna, and M. Castilla, “Hierarchical control of droop-controlled ac and dc microgrids – a general approach toward standardization”, *IEEE Trans. Ind. Electron.*, vol. 58, no. 1, pp.158- 172, Jan. 2011.

[3] J. M. Carrasco, L.G. Franquelo, J.T. Bialasiewicz, E. Galvan, R.C.

PortilloGuisado, M.A.M. Prats, J.I. Leon, and N. Moreno-Alfonso, “Power-electronic systems for the grid integration of renewable energy sources: a survey”, *IEEE Trans. Ind. Electron.*, vol. 53, no. 4, pp.1002- 1016, Aug. 2006.

[4] D. E. Olivares, A. Mehrizi-Sani, A. H. Etemadi, C. A. Canizares, R. Iravani, M. Kazerani, A. H. Hajimiragha, O. Gomis-Bellmunt, M. Saeedifard, R. Palma-Behnke, G. A. Jimenez-Estevez, and N. D. Hatziargyriou, “Trends in microgrid control”, *IEEE Trans. Smart Grid*, vol. 5, no. 4, pp.1905-1919, Jul. 2014.

[5] K. H. Ang, G. Chong and Y. Li, “PID control system analysis, design, and technology,” *IEEE Trans. Control Syst. Technol*., vol. 13, no. 5, pp. 1813– 1827, Sep. 2014.

[6] M. Kwon and S. Choi, "Control Scheme for Autonomous and Smooth Mode Switching of Bidirectional DC–DC Converters in a DC Microgrid," *IEEE Trans. on Power Electron.*, vol. 33, no. 8, pp. 7094-7104, Aug. 2018.

.

[7] A. Pirooz and R. Noroozian, "Model predictive control of classic bidirectional DC-DC converter for battery applications," *2016 7th Power Electronics and Drive Systems Technologies Conference (PEDSTC)*, Tehran, 2016, pp. 517-522.

[8] Y. Mei, L. Chen, X. Li and K. Sun, "Model predictive control method for cascaded bi-directional DC-DC converter applied to a stand-alone photovoltaic energy storage system," *2016 19th International Conference on Electrical Machines and Systems (ICEMS)*, Chiba, 2016, pp. 1-5.

[9] A. Merabet, K. T. Ahmed, H. Ibrahim, R. Beguenane, and A. Ghias, “Energy management and control system for laboratory scale microgrid based wind-pv-battery,” *IEEE Trans. Sustain. Energy*, vol. 8, no. 1, pp. 145–154, Jan. 2017.

[10] F. Nejabatkhah and Y. W. Li, “Overview of power management strategies of hybrid ac/dc microgrid”, *IEEE Trans. Power Electron.*, vol. 30, no. 12, pp.7072-7089, Dec. 2015